

2016

Computational Tracking of Shear-Mediated Platelet Interactions with von Willebrand Factor

Adam Ralph

Martin Somers

Jonathan Cowman

See next page for additional authors

Follow this and additional works at: <https://arrow.tudublin.ie/engschmecart>



Part of the [Biomedical Commons](#), and the [Mechanical Engineering Commons](#)

This Article is brought to you for free and open access by the School of Mechanical and Design Engineering at ARROW@TU Dublin. It has been accepted for inclusion in Articles by an authorized administrator of ARROW@TU Dublin. For more information, please contact arrow.admin@tudublin.ie, aisling.coyne@tudublin.ie, gerard.connolly@tudublin.ie.




This work is licensed under a [Creative Commons Attribution-NonCommercial-Share Alike 4.0 License](#)
Funder: Science Foundation Ireland

Authors

Adam Ralph, Martin Somers, Jonathan Cowman, Bruno Voisin, Emma Hogan, Hannah Dunne, Eimear Dunne, Barry Byrne, Nigel Kent, Antonio J. Ricco, Dermot Kenny, and Simon Wong

Computational Tracking of Shear-Mediated Platelet Interactions with von Willebrand Factor

ADAM RALPH,¹ MARTIN SOMERS,² JONATHAN COWMAN,³ BRUNO VOISIN,¹ EMMA HOGAN,¹ HANNAH DUNNE,³
EIMEAR DUNNE,³ BARRY BYRNE,² NIGEL KENT,⁴ ANTONIO J. RICCO,² DERMOT KENNY,³
and SIMON WONG ¹

¹Irish Centre for High-End Computing, IT Building, National University of Ireland, University Road, Galway, Ireland; ²Biomedical Diagnostics Institute, Dublin City University, Dublin 9, Ireland; ³Biomedical Diagnostics Institute, Royal College of Surgeons in Ireland, Dublin 2, Ireland; and ⁴School of Mechanical and Design Engineering, Dublin Institute of Technology, Bolton Street, Dublin 1, Ireland

(Received 27 April 2016; accepted 7 October 2016; published online 14 October 2016)

Associate Editors Baruch Barry Lieber and Ajit P. Yoganathan oversaw the review of this article.

Abstract—The imaging of shear-mediated dynamic platelet behavior interacting with surface-immobilized von Willebrand factor (vWF) has tremendous potential in characterizing changes in platelet function for clinical diagnostics purposes. However, the imaging output, a series of images representing platelets adhering and rolling on the surface, poses unique, non-trivial challenges for software algorithms that reconstruct the positional trajectories of platelets. We report on an algorithm that tracks platelets using the output of such flow run experiments, taking into account common artifacts encountered by previously-published methods, and we derive seven key metrics of platelet dynamics that can be used to characterize platelet function. Extensive testing of our method using simulated platelet flow run data was carried out to validate our tracking method and derived metrics in capturing key platelet-vWF interaction-dynamics properties. Our results show that while the number of platelets present on the imaged area is the leading cause of errors, flow run data from two experiments using whole blood samples showed that our method and metrics can detect platelet property changes/differences that are concordant with the expected biological outcome, such as inhibiting key platelet receptors such as P2Y₁, glycoprotein (GP)Ib and GPIIb/IIIa. These findings support the use of our methodologies to characterize platelet function among a wide range of healthy and disease cohorts.

Keywords—Platelet dynamics, Whole blood flow-based assay, Video fluorescence microscopy, Tracking algorithm.

INTRODUCTION

It is well established that cardiovascular disease is a major cause of mortality and morbidity, placing considerable financial burden on healthcare systems. Relevant to this disease, platelets play a key role in the pathogenesis of ischemic syndromes occurring in the vicinity of ruptured atherosclerotic plaques. Thus, understanding the intrinsic relationship between platelet activation states and their kinetic properties upon association with matrix proteins such as von Willebrand factor (vWF) under defined flow conditions (primarily the fluid shear rate at the platelet-vWF interface) provides physiologically relevant information directly relating to initial responses to vascular injury or damage.²⁰ Such interactions are shear stress-dependent, are influenced by blood flow conditions,^{8,12,22,23} are rapidly reversible, and result in start-stop (saltatory) platelet movements.^{1,2,8,9,12,22} Thus platelet thrombus formation is a dynamic process. In the arterial circulation, platelets tether to vWF via the glycoprotein (GP)Ib α receptor. As this receptor binds to vWF, it is stretched by the force of flowing blood, stimulating the platelet to initiate a complex signaling pathway modulated by other surface receptors (e.g. P2Y₁) and environmental factors. Ultimately this pathway leads to activation of the GPIIb/IIIa receptor and cross-linking of platelets occurs, leading to thrombosis. GPIIb/IIIa forms comparatively strong bonds to vWF surfaces, a key factor in the stable adhesion of platelets.

The characterization of platelet function through the use of technologies such as atomic force microscopy

Address correspondence to Simon Wong, Irish Centre for High-End Computing, IT Building, National University of Ireland, University Road, Galway, Ireland. Electronic mail: simon.wong@ichec.ie

provides useful insights into platelet binding interactions at fine spatial resolution.¹⁹ By extending this analytical concept to the microscopic level, Meyer dos Santos *et al.* examined platelet interaction with immobilized vWF and fibrinogen in a flow-based adhesion assay and developed computer software to count platelets that adhered stably to the surface and platelets that translocated.⁵ Inhibition of GPIIb α function resulted in a marked reduction in the observed number of translocating platelets, concordant with the expected physiological outcome. While this provided preliminary useful clinical insight, tracing platelet movements on such surfaces can be an error-prone process and there remain other quantifiable metrics reflective of platelet dynamics that have yet to be measured (e.g. the speed at which platelets translocate).

In a typical dynamic flow-based assay, platelets that bind to a vWF-coated surface can be observed to “stick” (stable adhesion) or “roll” (translocate in the direction of flow); in some cases the interaction is sufficiently weak that platelets disengage with the surface entirely. We can readily trace the positions of single platelets on the vWF surface over time, generating so-called “tracks” that are key for subsequent analysis (e.g. classification as being stationary or translocating, measurements of track length and speed). But a significant confounding factor in reliably determining platelet tracks using software is that platelets recruit and collide with one another, such events often involving multiple platelets, resulting in artifacts manifested as tracks appearing to merge and separate.

One common artifact is fragmentation of a single, real platelet track into observed multiple tracks owing to collision events. This track fragmentation phenomenon has been a common problem for several platelet “tracking algorithms” that have been previously described.^{6,7,21,24,26} From a clinical perspective, such sub-optimal tracking leads to ambiguity in the flow-based assay results and consequently any demonstrable outcome, including response to therapeutic agents (e.g. anti-platelet medication) and platelet function changes in response to acute thrombotic events.

Here, we describe the development and validation of a platelet-tracking algorithm based on a distance-weighted function that allows us to determine platelet tracks in whole blood flow-based assays, taking into account the track fragmentation phenomenon by effectively detecting when platelets collide and subsequently separate. We also derive and measure seven key metrics of platelet dynamics that are reflective of platelet function and biology. In order to verify the robustness and accuracy of these measurements, we test the output of our software against simulated,

“idealized” datasets where the true values are predetermined. Finally, we demonstrate the ability of this novel assay to detect changes in platelet function via observable changes across multiple derived measurements by *in vitro* inhibition of the P2Y₁, GPIIb α and GPIIb/IIIa receptors that play critical roles in thrombosis and platelet function. We also investigate the effect of platelet count on the extent of platelet-vWF interactions in our assay, in combination with other parameters. The software allows us to interrogate flow-based data from individual runs in less than 10 min, providing a rapid assessment of platelet function.

MATERIALS AND METHODS

Blood Sample Collection and In Vitro Administration of Platelet Receptor Inhibitors (MRS2179, AK2 and ReoPro)

This study was approved by the Medical Research Ethics Committee of the Royal College of Surgeons in Ireland and complied with the Declaration of Helsinki. For each donor, 10 mL of blood was drawn through a 19-gauge Butterfly needle into a polypropylene syringe (Becton–Dickinson, Oxford, UK) containing 3.2% (v/v) trisodium citrate dihydrate, selected as an anticoagulant. A total of 27 healthy volunteers who were free from medication known to affect platelet function for at least 10 days were selected for use in this study. Platelet counts were determined by enumeration with Sysmex-KX21 N hematology analyzer (Kobe, Japan).

In order to examine the effect of platelet count on platelet-vWF interactions in our flow-based system, a total of 12 blood donors were recruited with platelet counts that fall into three classes (5 donors with $150 \pm 20 \times 10^3 \mu\text{L}^{-1}$; 5 donors with $250 \pm 20 \times 10^3 \mu\text{L}^{-1}$; 2 donors with $350 \pm 20 \times 10^3 \mu\text{L}^{-1}$). Each blood sample was assayed in duplicate.

For subsequent *in vitro* platelet receptor inhibition experiments, any individual with abnormal platelet counts ($< 150 \times 10^3$ per microliter of blood) were excluded from the study.

We used the P2Y₁ receptor antagonist MRS2179 (Sigma, St. Louis, MO, USA) to examine its effects. Blood samples were taken from seven healthy individuals and assayed (in duplicate) on our flow-based system (see below) before and after incubation with MRS2179 (20 μM) for 10 min at 37 °C.

For the glycoprotein Ib α (GPIIb α) receptor, we used an inhibitory antibody, AK2 (AbD Serotec, Oxford, UK) to assess the outcome of its inhibition on our measured parameters. Blood samples were taken from four healthy individuals and treated with either control

IgG or incremental concentrations of AK2 (1.25, 2.5 and 5 μg). The blood samples were incubated for 10 min at 37 °C prior to conducting the flow-based dynamic platelet assay (see below). Each condition was assayed in duplicate.

For the glycoprotein IIb/IIIa (GPIIb/IIIa) receptor, we used the inhibitory antibody, ReoPro (Eli Lilly & Co., Indianapolis, IN, USA), to assess the outcome of its inhibition on our measured parameters. Blood samples were taken from four healthy individuals and treated with either control IgG or incremental concentrations of ReoPro (1.25, 2.5 and 5 μg). The blood samples were incubated for 10 min at 37 °C prior to conducting the flow-based dynamic platelet assay (see below). Each condition was assayed in duplicate.

Flow-Based Dynamic Platelet Assay

Platelet assays were conducted using a previously-characterized microfluidic flow-based system and experimental methodology that measures dynamic platelet-vWF interactions in microliter volumes of unmodified anticoagulated whole blood under established arterial shear conditions.^{10,13} It includes a parallel plate flow chamber consisting of a 25 \times 55 mm polymethylmethacrylate (PMMA) top plate with 1/16 mm polypropylene inlet and outlet connectors (Ensinger Plastics, UK), an acrylic adhesive gasket (Adhesives Research, Limerick, Ireland) defining the microfluidic channel (2 mm wide, 50 μm high, 35 mm long), and a 24 \times 50 mm bottom glass microscope coverslip (Bio-World, Dublin, OH, USA). Purified human vWF (courtesy of Robert Montgomery, Blood Research Institute, Milwaukee, WI, USA) is immobilized on the glass coverslip that forms the base of the microfluidic flow channel.

Blood samples are incubated with a lipophilic fluorescent dye, DiOC6 (1 μM DiOC6; Invitrogen, Carlsbad, CA, USA) at 37 °C for 10 min for visualization of platelets against the background of flowing whole blood. These are then drawn through bio-compatible platinum-cured silicone tubing (Nalgene, Thermo Fisher Scientific, Denmark) into the flow channel using a Nemesys syringe pump (Cetoni GmbH, Korbussen, Germany) at a controlled flow rate of 75 $\mu\text{L min}^{-1}$, resulting in the physiologically relevant arterial shear rate of 1500 s^{-1} (as established by Kroll *et al.*¹¹) and shear stress of 6 Pa (6 N m^{-2}) at the wall where platelet-vWF interactions occur. Approximately 200 μL of blood is perfused through the device for each flow run analysis.

Platelets are imaged by video fluorescence microscopy as they tether, adhere, roll, and form thrombi on the bottom vWF-coated surface. The key output from this procedure is a time-sequenced set of grayscale

images or frames, captured at a rate of 30 frames per second (fps), of a 133 \times 133 μm^2 section of the surface. Importantly, only those platelets that interact with the vWF surface are captured by the imaging software (Metamorph[®] Image Analysis Software, Molecular Devices, LLC, Sunnyvale, CA, USA), because those that move with the flowing blood move much too rapidly to be imaged at 30 fps. Our primary focus is on monitoring the early stages of platelet adhesion and interaction over 16.7 s of each flow run experiment (equivalent to 500 frames), before large-scale platelet aggregation and thrombus formation occurs.

Image Analysis and Tracking Algorithm

Image processing is conducted using the MATLAB Image Processing Toolkit (MathWorks, Natick, MA, USA). Each image (out of 500) captured from a flow run experiment first undergoes background reduction. For each frame the background image is constructed by averaging over a 30 \times 30 pixel window over each image pixel. The background is then subtracted from the original image and the edges removed. This background-subtracted image is masked using the MATLAB functions *graythresh* and *im2bw*, converting the grayscale image into a black and white image where the threshold is determined analytically per image/frame using Otsu's method¹⁶ that minimizes the interclass variance of the black and white pixels, i.e. the masking threshold is not defined explicitly but can change from one frame to the next. Thus platelets appear as white shapes on a black background. It was then possible to detect and record the (*x,y*) centroid position and approximate size of each platelet on every frame using the MATLAB *regionprops* function. Shown in Fig. 1 is an original grayscale image captured by the camera that has subsequently been subjected to the background subtraction and masking process, resulting in a black and white image annotated with the centroid positions. Next, a platelet track can be constructed by identifying the same platelet from one frame to the next, allowing some displacement in its position (see below for empirical limits for this displacement), and recording any change in (*x,y*); this is then repeated for subsequent frames. However, there are a number of confounding factors in this process. Platelets tend to move in a saltatory fashion that makes it difficult to predict their positions from one frame to the next. They can be observed to vary in size and shape over time, in part as a result of actual changes in size or morphology, and in part because platelets are not spherical, hence their 3D orientation when projected on a 2D image impacts the perceived area and shape. Finally, platelets collide with one

another and separate over time, making it extremely difficult to trace the true trajectories of individual platelets for all but the most trivial cases such as “solitary” platelets; typically we observe a significant number of platelet collision and separation events in real experiments.

In our tracking algorithm, we construct a weighted distance matrix based on a track’s position and the locations of all other platelets on the next frame. The weighting factor gives preference to platelet movements in the direction of blood flow, as opposed to cross-stream movements, hence each distance (d) is computed using both the Euclidean (x,y) displacement and its angle (θ), measured in radians, from the flow

direction (where $\theta = \arctan(\Delta x/\Delta y)$, $-\pi \leq \theta \leq \pi$) according to the following formula:

$$d = \left(\sin\left(\frac{\theta}{2}\right)^2 + 1/2 \right) \times \sqrt{(\Delta x^2 + \Delta y^2)} \quad (1)$$

In Eq. (1), the minimum weight factor is 0.5, when $\theta = 0$ or in other words the (potential) movement is directly downstream in the direction of flow ($\Delta x = 0$; $\Delta y > 0$). The maximum weighting factor is 1.5 when $\theta = 180^\circ$ (or π radians), a movement directly against the direction of flow ($\Delta x = 0$; $\Delta y < 0$). Cross stream movement ($|\Delta x| > 0$; $\Delta y = 0$) has a weighting factor of 1 equally in either direction as determined by $\left(\sin(\pi/4)\right)^2 + 1/2$.

Each track is then extended by assigning it to a platelet in the next frame, if possible, by applying a set of rules in conjunction with the weighted distance matrix (Table 1). Critically, we monitor complementary changes in platelet areas together with positional information from the weighted distance matrix to detect whether two or more platelets have merged or separated. The output from the tracking algorithm consists of a list of tracks with (x,y) positions and areas (occupied by the platelets in each frame) over time, detailing platelet movements over the 500 frames of the experiment.

Hard limits (similar to y_c as outlined by Lincoln *et al.*¹³) were put in place to prevent recorded tracks from extending over distances that are considered physically impossible, i.e. if $|\Delta x| > 5.2 \mu\text{m}$ or $\Delta y > 5.2 \mu\text{m}$ upstream or $\Delta y > 26.0 \mu\text{m}$ downstream, the track extension is rejected. Platelets that move more than these limits will be considered as new platelets, thus terminating the original track and commencing a new one. The limits were determined empirically from visual inspection of over 60 whole blood flow experiments from normal individual donors and patients with stable and acute cardiovascular disease (unpublished data).

Finally, after all of the tracks are generated, a subset may be rejected based on two criteria: if a track persists for ≤ 10 frames or if the platelet size for a particular track is less than approximately $3 \mu\text{m}^2$. The first criterion was implemented to remove fragmented tracks that are likely to be artifacts and would therefore skew the resulting summary statistics; some level of track fragmentation is unavoidable. The second removes artifactual tracks that likely result from partial staining of platelets by the fluorescence dye, as the area of even the smallest platelet is at least $4 \mu\text{m}^2$. Shown in Fig. 2 is a visual plot of all the valid platelet tracks from a real flow run.

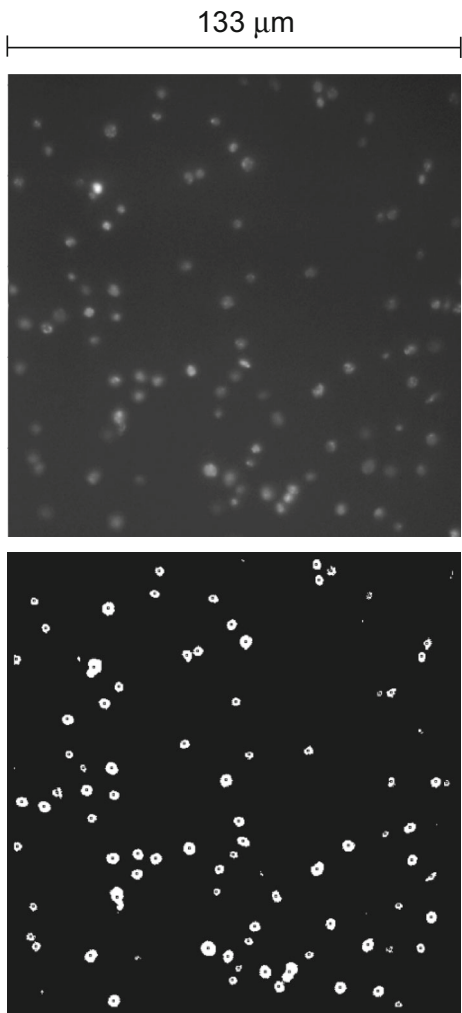


FIGURE 1. Single image/frame captured by the camera from a flow run (top). After background subtraction and the masking process, it becomes a black and white image (bottom), where platelets appear as white objects against a black background. Black dots in the middle of platelets indicate centroid positions.

TABLE 1. Rules under which new platelets are assigned to previously recorded tracks.

Scenario	Criteria	Outcome
1	R_a and S_i are closest to each other	Track extended unambiguously
2	R_a and R_b are closest to S_i , with a suitable increase in size (area) of S_i	Two or more platelets merge into a single object on the next frame
3	S_i and S_j are closest to R_a , with R_a detected as a merged platelet with size approximately equal to S_i and S_j combined	Two or more merged platelets split into multiple objects on the next frame
4	Same as 3 but R_a is not deemed to be a merged platelet	Apparent single platelet splits into two objects on the next frame. This means that the original object was in fact two stacked platelets
5	All suitable new platelets have been assigned to existing tracks	Tracks cannot be extended; any un-extended tracks means that the tracked platelets have disappeared from view
6	All the suitable recorded tracks have been extended	Remaining platelets in the next frame form the beginning of new tracks

For six scenarios, based on the weighted distance matrix, R indicates the x,y centroid coordinates of a platelet at the end of an existing, recorded track at a particular frame; S indicates the x,y centroid coordinates of a platelet on the next frame to be assigned. Subscripts (a,b,i,j) denote the identities of different objects detected.

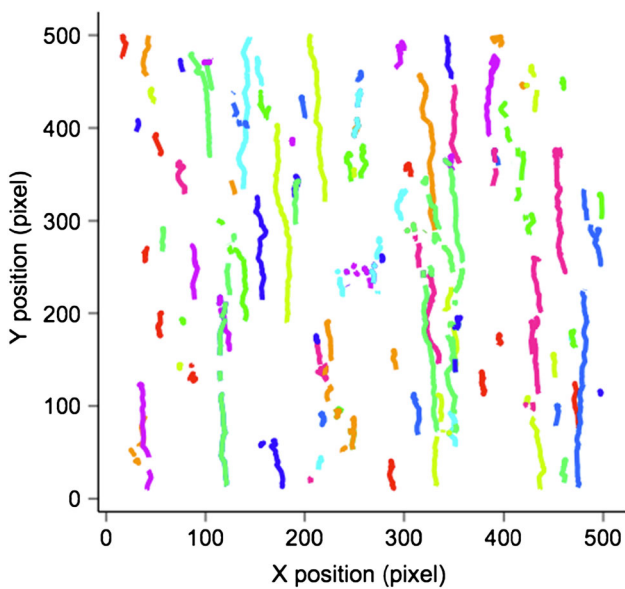


FIGURE 2. Visual representation of valid platelet tracks that have been detected using the tracking algorithm. Platelets generally translocate in the direction of flow (downwards).

Derivation of Platelet Dynamics Metrics

For analysis and comparison of flow run experiments, we derive and compute a total of seven metrics that reflect platelet dynamics and function. The metrics, how they are derived and biological relevance are summarized in Table 2. The accuracy of these metrics is then assessed using simulated datasets (see below).

Construction of Simulated, “Idealized” Datasets

Images from a number of different flow run experiments were selected to determine a range of empirical values for platelet size, translocation speed and distance. Using these parameters, different sets of simu-

lated flow run images were generated using MATLAB (see example frame in Fig. 3). These are then analyzed by our image processing and tracking algorithm to determine the accuracy of individual metrics measured, by comparison with known values of the simulated datasets.

For each simulated dataset, four variables were fixed (see Table 2 for definitions of these variables): the number of tracks being simulated (50, 100, 150, 200, 250, 300, 350, 400), the fraction of stably-adhered platelets (10, 20, 30%), the translocation speed (0.5, 1.0, 1.5 pixels per frame) and the translocation distance (50, 100, 150 pixels). For each combination of the above four variables, three runs were generated that are then analyzed using our tracking algorithm and metrics computed. We use the term “error” in the specific context of inaccuracies in the values of our derived metrics when compared to the “true” values that are known, i.e. those are used as input to our simulation. For example, if 55 stably-adhered platelets were computed from a simulated dataset with a true value of 50 stably-adhered platelets, this results in an absolute error of 10%, caused by mistracking events. As a control, several runs were generated with no merging or separation events. These runs were found to be “error free” and thus gave the expected values for each variable (results not shown), serving as controls and a standard test method for development of the algorithm.

Each simulated flow run is comprised of tracks with known trajectory profiles, which were then used to generate the images or frames. A roughly circular object was placed on a sequence of frames to represent a single platelet track, under the condition that platelets do not overlap one another initially but are allowed to merge and separate in subsequent frames. On the first frame of each run, 25 platelets were

TABLE 2. Definition and derivation of seven platelet dynamics metrics from the analysis software, along with biological relevance of the metrics.

Flow run metric	Derivation	Biological relevance
<i>Total number of tracks</i>	Number of unique platelet tracks observed over 500 frames, after rejection of likely artifacts (transient or partial platelets)	Indicative of the overall extent of platelet-vWF interactions (mediated by GPIb, in conjunction with adhesion rate)
<i>Number of translocating platelets</i>	From the total number of tracks, a platelet is classified as translocating if it has moved $1.5\times$ its average radius as an observed single platelet over its lifetime (i.e. distance moved when merged with another platelet is ignored). Otherwise, the platelet is classified as stably-adhered	Indicative of overall rolling/translocating activity on the surface after initial platelet-vWF interaction (mediated by GPIb receptor activity). Higher proportions of such platelets indicates reduced "stickiness" of the platelet population
<i>Number of stably-adhered platelets</i>		Indicative of the level of initial platelet interaction with vWF (mediated by GPIb receptor activity) followed by stable adhesion (mediated by GPIIb/IIIa) to the surface
<i>Weighted median speed</i> ($\mu\text{m s}^{-1}$)	Instantaneous platelet movements (from one frame to the next) are smoothed over a moving 5-frame window (to reduce the effect of platelet wobble). The weighted median speed is the 50% <i>weighted</i> percentile of the sample comprised of all instantaneous speeds from tracks representing translocating platelets; excludes artificial movements (see "Results" section)	An increase in speed may reflect reduced signalling within the platelet that leads to slower activation of GPIIb/IIIa that mediate stable adhesion, and <i>vice versa</i>
<i>Mean translocation distance</i> (μm)	Mean of all distances covered by translocating platelets after removal of artificial movements. To calculate each track distance, the frame-to-frame x and y displacements (Δx and Δy) are summed separately (including sign), then squared and added	Similar to speed in that increased distances reflect reduced signaling leading to slower activation of GPIIb/IIIa, and <i>vice versa</i>
<i>Surface coverage</i> (%)	Percentage of the sum of platelet-occupied areas on a particular frame (area of 512×512 pixels ²). Two variations were used: the surface coverage on the last frame and the difference in surface coverage between the first and last frame	This parameter relates to the propensity of platelets to interact with the vWF surface and the level of stable adhesion during the time-frame of the observation window. Higher surface coverage, examined in conjunction with other parameters such as the number of translocating/stably-adhered platelets, may indicate increased interaction mediated by GPIb and/or stable adhesion mediated by GPIIb/IIIa
<i>Adhesion rate</i> (slope)	An estimate of the rate at which new tracks appear on the surface, calculated from the number of platelets observed per frame and fitted to a linear model	Increase in the rate of adhesion indicates greater extent of initial platelet-vWF interaction mediated by GPIb, and <i>vice versa</i>

placed randomly, followed by gradual addition of platelets at regular intervals until the expected number of tracks has been added by the last frame. Since platelets were placed randomly in areas where they would not overlap with other platelets initially, any deviations from the expected number are expected to be the result of mistracking owing to platelet merging/separation events. Each translocating platelet moves in an identical manner for a given dataset, i.e. it translocates for 50/100/150 pixels at 0.5/1.0/1.5 pixel per frame and then adheres stably to the surface. Stably-adhered platelets do not move at all after attachment to the surface. The translocating platelets move only in the direction of the flow with no restrictions on the number of mergers and separations after their initial adherence on the surface.

SYSTEM CALIBRATION

A conversion factor was determined so that all measurements from the fluorescence microscopy system could be quantitatively related to the physical movements of platelets within the parallel plate flow chamber, i.e. distances in pixels were converted to μm . Based on a previously described protocol,¹⁴ we used microcontact printing to generate an array of fluorescently-labelled fibrinogen spots ($6 \mu\text{m}$ in diameter, separated in all planes by $\sim 15 \mu\text{m}$, and labelled with fluorescein isothiocyanate, FITC) on glass slides, which were subsequently used to determine the field of view and conversion factor. Due to the microcontact-printing process, the level of error is in the range of 1–2%.¹⁷

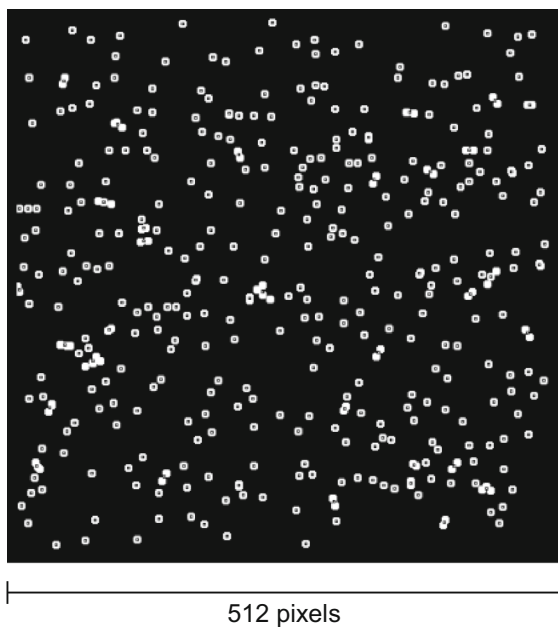


FIGURE 3. Example of a single frame from a simulated dataset used to validate the tracking process. The centroid of each simulated platelet (white objects) is marked with a black dot.

STATISTICAL ANALYSIS

The plots were produced by the statistical package R¹⁸ with the ggplot2 package.²⁵

RESULTS

Artificial Movement

When examining platelet motion in flow run experiments that involve interactions with a protein coated surface, several sources of systematic error must, in general, be addressed. When platelets merge and separate, there is an apparent movement of the centroids of all platelets involved that may be incorrectly interpreted as physical translocation, because merged platelets are identified as a single object (with a single centroid) on any particular frame. An example of artificial movement is presented in Fig. 4, where platelets B and C merge into a single observed object, platelet D, from one frame to the next. The centroids of both platelets B and C have apparently moved to the region where they merge and overlap, resulting in an “artificial movement” for their respective platelet tracks. This artificial movement, if not accounted for, can affect the values of platelet speed and distance traveled, especially when larger clusters of platelets merge. Hence, our algorithm is designed to detect such merging/separation events and to discount such artificial movements for subsequent derivation of metrics.

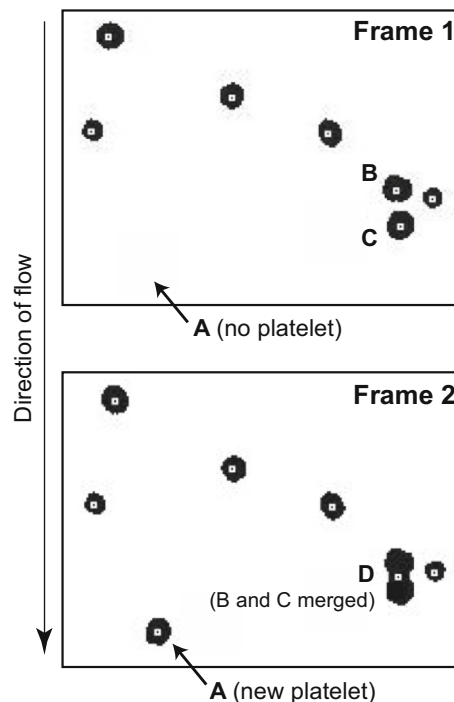


FIGURE 4. Two consecutive frames of masked images. Detection of a new platelet (A) at Frame 2; platelets B and C are two platelets in Frame 1 that collides and detected as a single merged object (D) in Frame 2. The white dots inside each platelet indicate their centroid locations.

Shown in Fig. 5 are the trajectories (only in the y direction) of a select number of platelet tracks over time from real flow runs that highlights in more detail cases of artificial movements where the y position of several platelet tracks can be observed to fluctuate backwards (against the flow) and forwards, resulting in apparent movement that are caused by merging/separating events. Indeed these artificial movements can account for large proportions of the higher instantaneous frame-to-frame motion that are recorded (Fig. 6); for a typical flow run about half of such motions (equivalent to frame-to-frame speeds of over $4 \mu\text{m s}^{-1}$) can be attributed to such artificial movements. While the majority of instantaneous motions recorded is below $4 \mu\text{m s}^{-1}$ (see Online Resource 1), such obvious and detectable erroneous motions are removed using our tracking algorithm.

A second potential cause of artificial movement is platelet “wobble”. The 2D-imaged shapes of platelets can change from one frame to the next because the masking threshold level, which is determined analytically per frame (see “Materials and Methods” section), can change or the (non-spherical) platelets change orientation relative to the imaging plane; they can even change shape physically while translocating. Such changes cause small fluctuations and ambiguity in each platelet’s centroid position, affecting the frame-to-

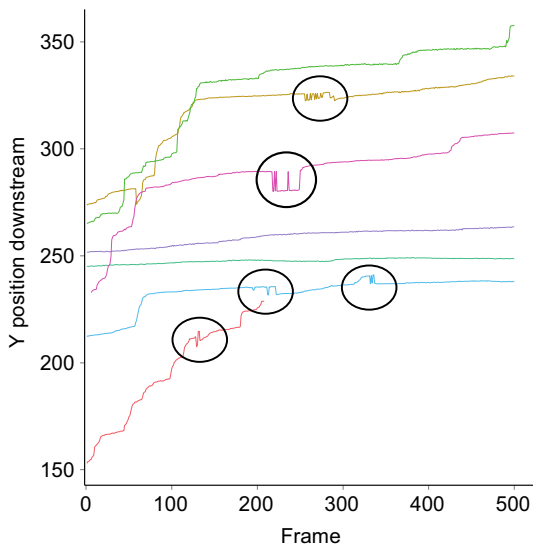


FIGURE 5. Plot of a select number of platelet tracks (in the Y direction only, same as the flow) over frames 1 to 500 of a flow run. Black ellipses highlight artificial movements where the Y coordinate of the relevant platelet tracks can be observed to fluctuate forwards and backwards (against the flow).

frame or instantaneous speeds that are measured for each track and subsequently aggregated to generate summary statistics. Hence, our algorithm implements a 5-frame sliding window (moving average) when computing each instantaneous speed to ameliorate the effects of platelet wobble.

Determination of Systematic Error

Expectedly, the main influence on the degree of errors for all of the derived metrics is the number of platelet tracks observed over 500 frames, which is correlated with the number of merging and separating events and, hence, incidences of mistracking. For this reason, the mean absolute errors for a range of simulations with seven different numbers of platelet tracks are presented in Fig. 7, where the number of simulated tracks is fixed and the absolute errors are calculated and averaged for different configurations of stably-adhered platelets and translocation speed/distance (see Table 2 for their definition and derivation). Only five out of the seven metrics are shown in Fig. 7; the two metrics that were not shown are: (i) number of translocating platelets, which is directly correlated with the number of stably-adhered platelets, a metric examined below, and (ii) surface coverage, a metric computed in a way equivalent to counting white pixels against a black background, i.e. area of the observed surface occupied by platelets at a particular frame; there is no meaningful method to simulate or calculate error rates for this metric because the simulations are

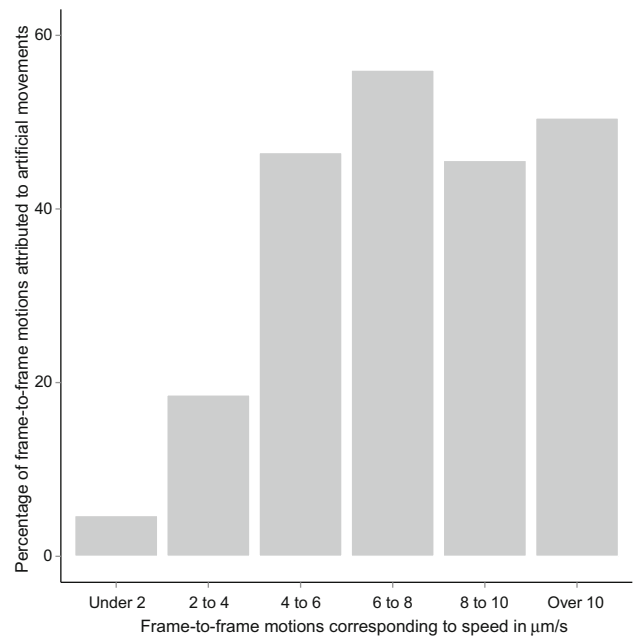


FIGURE 6. Proportions of frame-to-frame motions that can be attributed to artificial movements, caused by merging/separation events and removed by the tracking algorithm.

pure black-and-white images, unlike real fluorescence microscopy video frames that are grayscale, requiring a threshold to be set for what is “white” and what is background.

As anticipated, the mean absolute errors are indeed correlated with the number of tracks, confirming our hypothesis that higher incidences of merging/separation events is the leading cause for uncertainty in the derived metrics. However, it can be seen that our metrics are differentially affected by increasing numbers of tracks, as examined in more detail below.

Number of Tracks

Here we compare the computed number of tracks from our algorithm against the actual number of tracks in different simulations. Higher error rates were observed as the number of tracks increases (Fig. 7), but the magnitudes of the errors tend to be low (mean absolute error of 1.6% at the highest number of 400 simulated tracks). There is a tendency to over-estimate the number of tracks, as some level of track fragmentation is unavoidable due to more complex merging/separation events as the number of tracks increases.

Stably-Adhered Platelets

Figure 8 shows the error in the number of stably-adhered platelets computed from simulations of

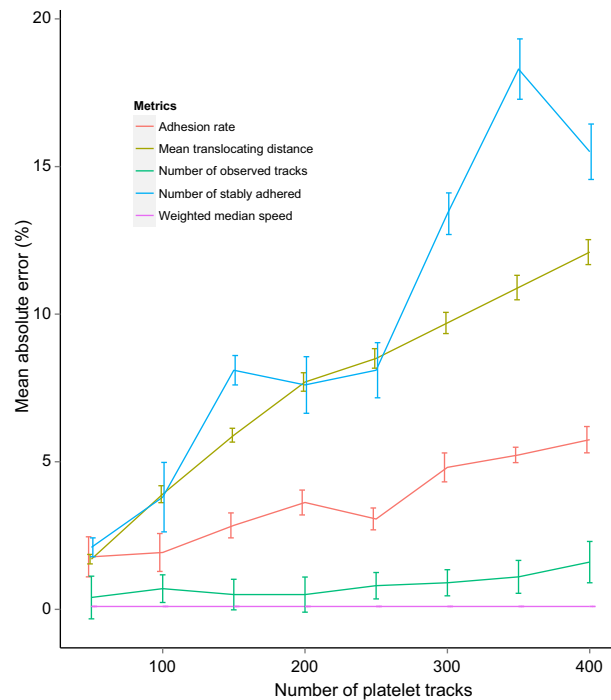


FIGURE 7. Mean absolute errors for different metrics, calculated for varying numbers of (simulated) tracks. Error bars indicate standard error of the mean.

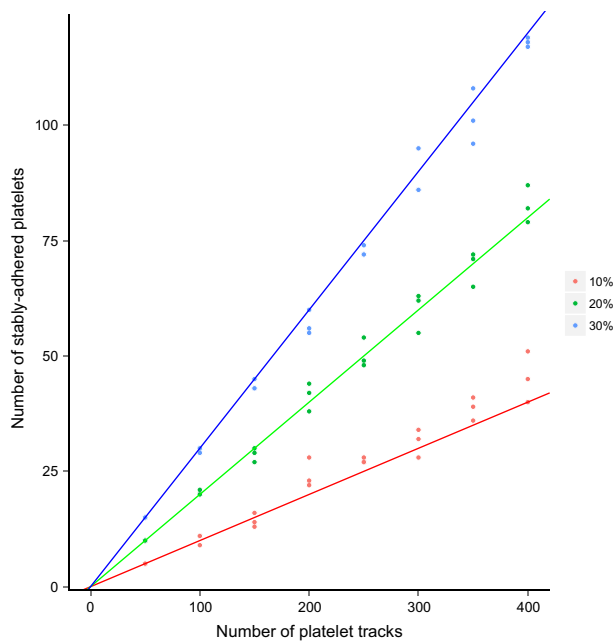


FIGURE 8. Number of stably-adhered platelets detected by the algorithm (in triplicate runs) vs. expected number of platelet tracks. Straight lines indicate the expected number of stably-adhered platelets from the simulations.

different numbers of tracks and pre-determined fractions of such platelets (10/20/30%). Expectedly, the magnitude of the error increases with the number

of tracks, up to ~18% at 350 tracks (Fig. 7), and in most cases the errors are due to over-estimates of the actual values. This is again a likely artifact of track fragmentation, e.g. if the track of a translocating platelet is mis-interpreted as several independent tracks by the software, some of the fragmented tracks would be deemed (justifiably) as a stably-adhered platelet because translocating platelets in our simulation, like platelets observed in real experiments, do not move constantly.

Weighted Median Speed

In order to capture the overall translocation speeds of platelets as a single scalar metric, we use the *weighted* median or 50% weighted percentile method. This is computed from a sorted list of all instantaneous speeds (v_1, v_2, \dots, v_n) observed from translocating platelet tracks in an experiment, and finding the element v_k , representing the *weighted* median speed, that

satisfies: $\sum_{i=1}^k v_i < \frac{1}{2} \sum_{i=1}^n v_i$ and $\sum_{i=1}^{k+1} v_i \geq \frac{1}{2} \sum_{i=1}^n v_i$. The ratio-

nale behind this method is that it should reduce the effect of extreme outliers that are typically observed in distributions of instantaneous speeds (see Online Resource 1).

The observed errors for the weighted median speed were very low (0.1%) and appear to be insensitive to higher numbers of tracks (Fig. 7). But if the mean,

rather than the 50% weighted median, were used instead as an indication of speed, error rates of 5–10% would be observed for the same set of simulated runs (data not shown). These results suggest that the weighted median method is preferable to the mean in providing an indicative overall speed of translocating platelets in a flow run.

Mean Translocation Distance

For the analysis of mean translocation distances, we simulated platelets that translocated 50/100/150 pixels while keeping their speeds constant (one pixel per frame) when moving. The largest errors observed for the mean distance is on the order of about 12% (Fig. 7).

Adhesion Rate

As this is a straight-forward process of capturing the rate at which platelets appears in our observation window, we observed relative small error rates of 2–5% in determining this parameter from our simulated flow runs (Fig. 7).

Utility of the Tracking Algorithm and Metrics in Biological Systems

To demonstrate the utility of our algorithm and derived metrics in biological systems, we first examined the ability of the algorithm to detect varying extent of platelet binding interactions with vWF due to differences in platelet count. A total of 12 blood donors were recruited whose platelet counts can be separated into three classes (5 donors with $150 \pm 20 \times 10^3 \mu\text{L}^{-1}$; 5 donors with $250 \pm 20 \times 10^3 \mu\text{L}^{-1}$; 2 donors with $350 \pm 20 \times 10^3 \mu\text{L}^{-1}$). Expectedly, there is a clear correlation between platelet count and the number of observed tracks in our assay as shown in Fig. 9, where data for the other measured parameters are also plotted. As the number of tracks increases with platelet count, the numbers of stably-adhered platelets as well as translocating platelets also increase, but the ratio remains more or less the same as do other parameters such as translocation speeds and distances. The indications from the measured parameters is that while there are simply more platelets interacting with vWF at higher platelet counts, the “behavior” of the platelets themselves are largely similar across individuals with different platelet counts.

We then set up a series of experiments to assess our ability to detect the effects of inhibiting key platelet receptors *in vitro*. Our first experiment involved treatment of donor blood with MRS2179, a selective antagonist of the ADP receptor P2Y₁, which is involved in platelet shape change and initiation of

platelet aggregation. Furthermore, it has been shown that compounds that inhibit the P2Y₁ platelet receptor affect the shape of the platelet when it binds to vWF attached to a surface and, hence, such compounds also affect the translocation speed, i.e. inhibition of the P2Y₁ receptor causes platelet to translocate faster, and subsequently reduced aggregation.¹⁵ Figure 10 shows the effect of MRS2179 across the seven parameters compared with controls, including the expected increase in platelet translocation speeds for blood treated with the P2Y₁ antagonist. While this observed increase in speed is somewhat weakly significant ($P < 0.05$, paired *t* test), we observe no significant differences in the other parameters.

In the subsequent experiment we examined AK2, an antibody that inhibits the function of the GPIIb/IIIa receptor that is critical for initial platelet-vWF interaction. Figure 11 shows the effect of increasing concentrations of AK2 on the seven parameters we measure. Expectedly, *in vitro* addition of AK2 reduced the number of tracks observed, indicating the expected decreased levels of platelet-vWF interactions proportional to the dose of AK2; at the highest 5 μg dose of AK2, platelet-vWF interactions are completely inhibited where no platelet tracks can be observed in any of the flow runs (hence not shown in Fig. 11). Similarly, this blocking of initial platelet-vWF interactions caused corresponding drops in the number of stably-adhered/translocating platelets as well as marked decreases in adhesion rate and surface coverage. On increasing the dose of AK2, we also observed increases in translocating speed and distances. These results are concordant with reduced signaling within the platelets, caused by GPIIb/IIIa inhibition, which led to slower activation of GPIIb/IIIa and hence increased time for stable adhesion to vWF.

Finally, we examined *in vitro* administration of ReoPro, a GPIIb/IIIa inhibitor that is critical for the formation of strong platelet-vWF bonds, i.e. inhibition of this receptor do not prevent initial platelet-vWF interaction like in AK2, but GPIIb/IIIa-inhibited platelets should behave in a more “slippery” manner with higher translocation speeds/distances with reduced levels of stable adhesion. Figure 12 shows the effect of ReoPro on all seven parameters we measure from the assay. As expected we see a consistent reduction in stably adhered platelets across all doses of ReoPro, but the number of translocating platelets, translocating speeds and distances all increased with higher doses; at 2.5 to 5 μg of ReoPro, the effect of GPIIb/IIIa inhibition appeared to be saturated. Meanwhile, initial platelet-vWF interactions do not appear to be affected by ReoPro as there is no reduction in the number of tracks observed nor significant differences

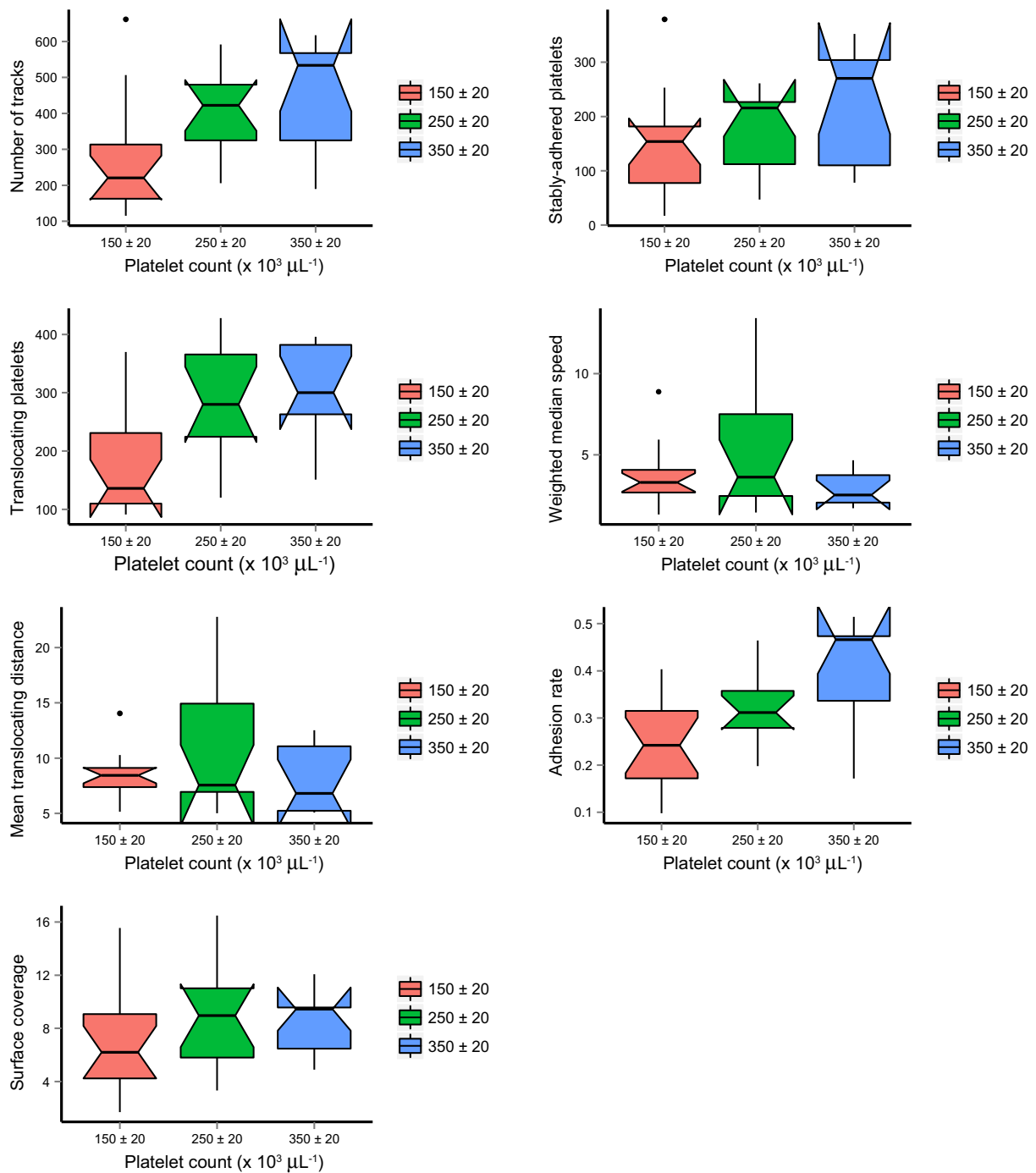


FIGURE 9. The seven panels show each of the metrics plotted against three cohorts of (healthy) individuals with platelet counts that can be divided into three classes ($n = 12$). Boxplots are shown for each group with the horizontal bar at the median. The limits of each box shows the inter-quartile range. The “notches” on each box indicates the 95% confidence interval on the median. The black dots represent outliers in the group and the vertical lines are valid limits of the data.

in the adhesion rates across all ReoPro doses and control. The observation that the number of tracks has actually increased with higher ReoPro concentration is not by itself evidence of increased initial platelet-vWF interactions (i.e. that we are seeing the

opposite effect of AK2), in this case the trend can be explained by higher levels of platelet “traffic” that can be observed, as platelets translocates faster and further, more of them roll into and out of our fixed window of observation.

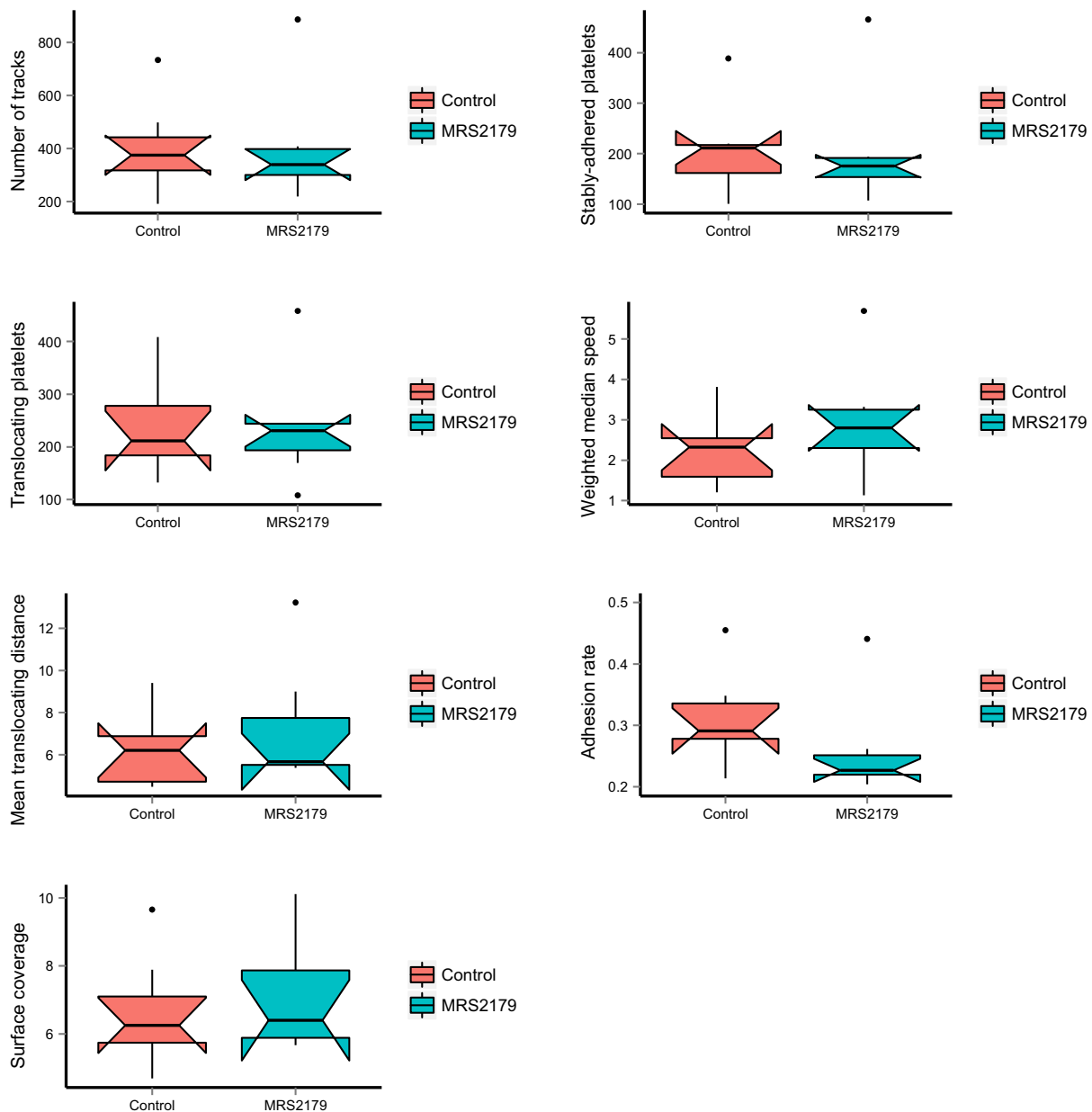


FIGURE 10. The seven panels show each of the metrics plotted against treatment with MRS2179 (20 μ M) relative to control ($n = 7$). Boxplots are shown for each group with the horizontal bar at the median. The limits of each box shows the inter-quartile range. The “notches” on each box indicates the 95% confidence interval on the median. The black dots represent outliers in the group and the vertical lines are valid limits of the data.

DISCUSSION

The imaging of shear-mediated dynamic platelet behavior interacting with surface-immobilized vWF has tremendous potential in characterizing changes in platelet function, which could then be adapted for a variety of clinical diagnostic purposes, e.g., determining risk of thrombosis or bleeding in response to antiplatelet therapeutics. While there is abundant literature on platelet-vWF interactions in general,³

most of the studies so far (based on real-time imaging of dynamic platelet behavior) have focused on single characterization parameters such as incidence of stable adhesion vs. translocation.⁵ We argue that significantly more powerful ways to characterize platelet behavior, both quantitatively and qualitatively, come from analysis of multiple parameters (such as the metrics in Table 2) that are determined from a single assay. It is also important to emphasize that the assay employed in this study, including the specific

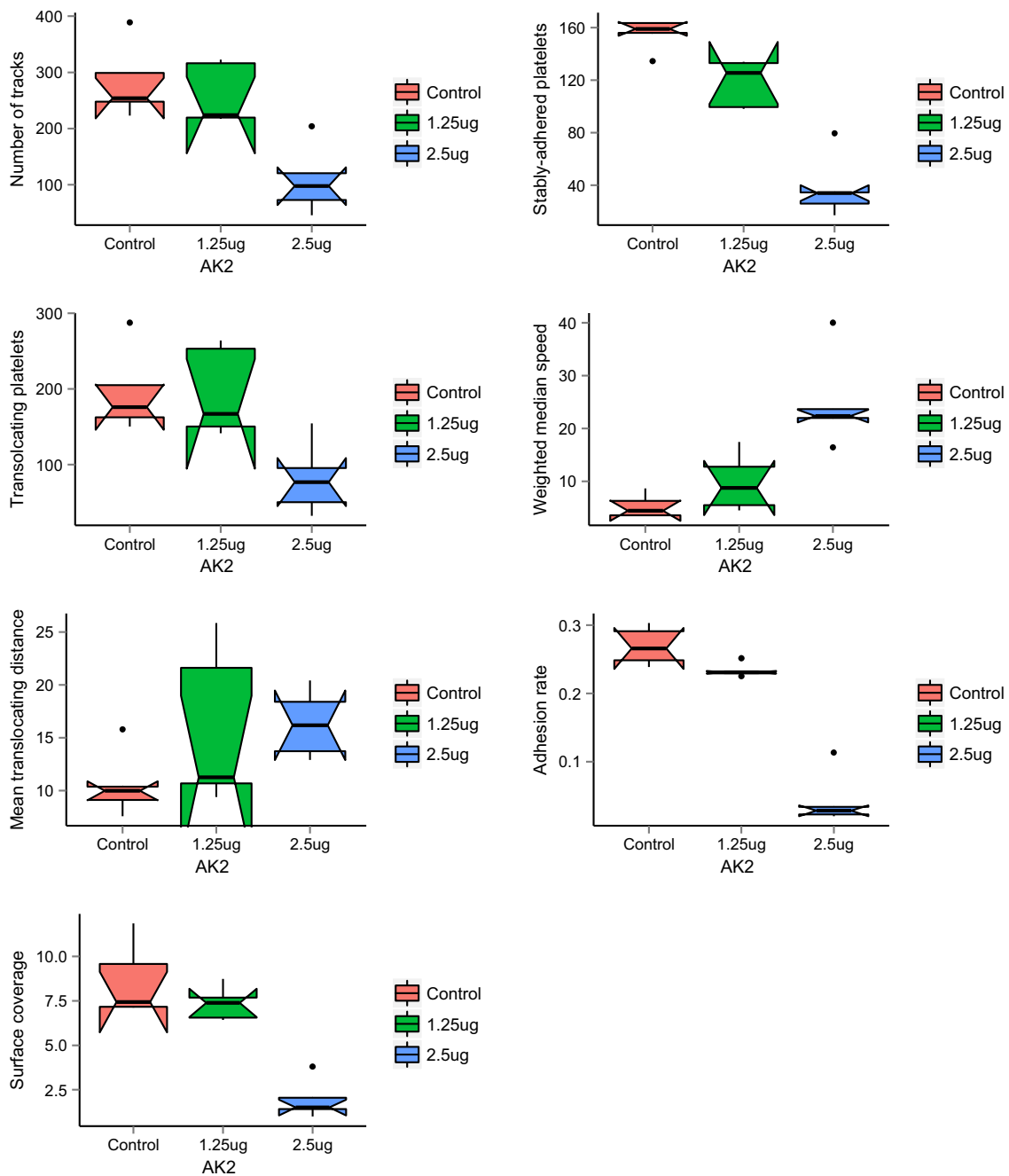


FIGURE 11. The seven panels show each of the metrics plotted against doses of AK2 relative to control ($n = 4$). Boxplots are shown for each dose level with the horizontal bar at the median. The limits of each box shows the inter-quartile range. The “notches” on each box indicates the 95% confidence interval on the median. The black dots represent outliers in the group and the vertical lines are valid limits of the data. Experiments using $5 \mu\text{g}$ doses of AK2 were carried out but not plotted here as there were no detectable platelet tracks in any of those flow runs.

experimental conditions, have been extensively tuned to mimic arterial wall damage (e.g. the use of a single physiologically relevant flow/shear rate¹¹) and designed to minimize blood sample perturbation (i.e. requirement of sub-milliliter volumes of whole blood rather than re-constituted platelet-rich plasma).^{10,13} We have also derived our measured parameters using the assay

to focus on the early events of arterial thrombosis, i.e. initial interactions of platelets with vWF over a time window of 16.7 s, rather than downstream events such as secondary platelet recruitment, more large-scale aggregation and thrombus formation.

A key problem we have identified from the outset is reliably tracking complex platelet translocation or

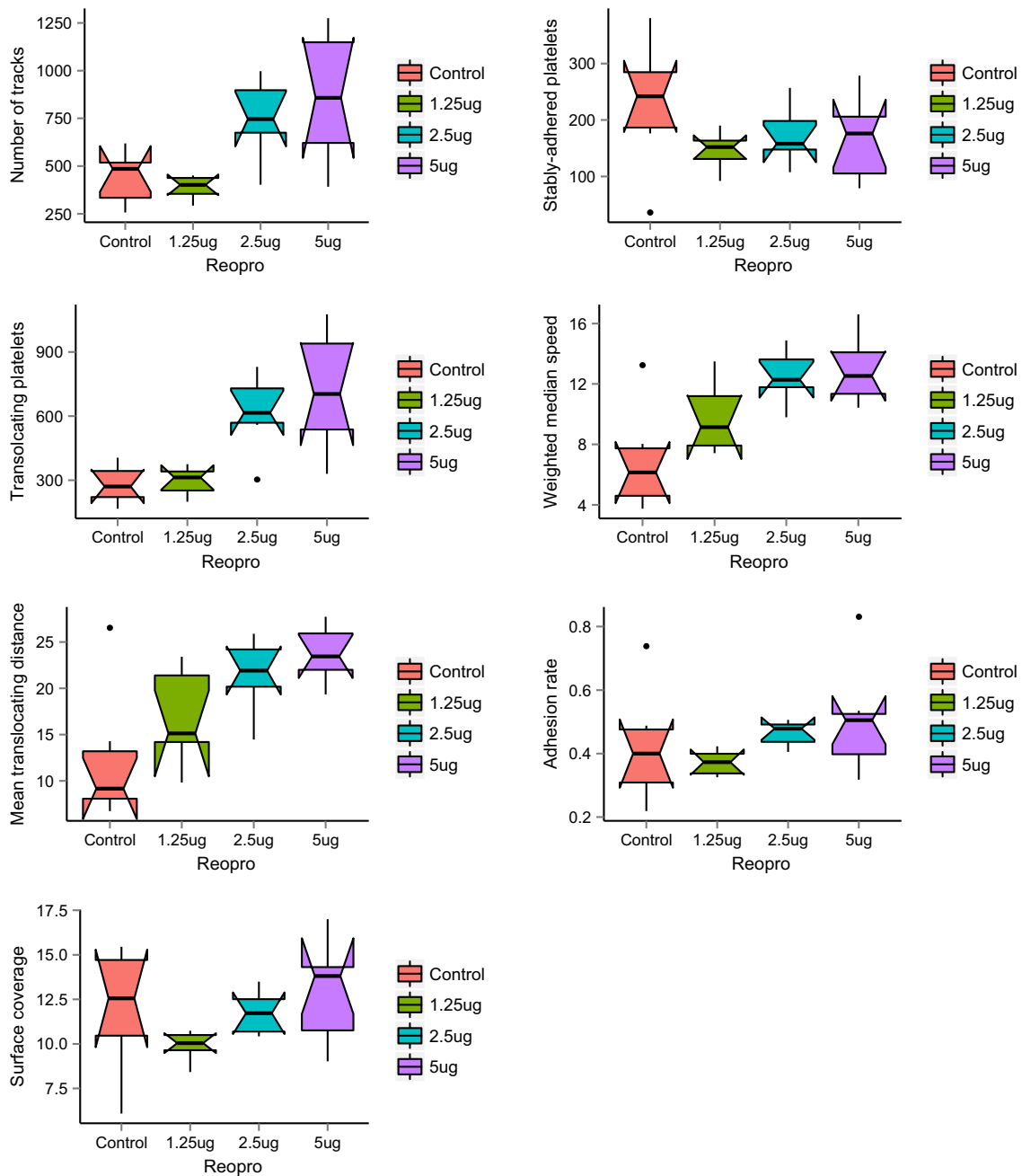


FIGURE 12. The seven panels show each of the metrics plotted against doses of Reopro relative to control ($n = 4$). Boxplots are shown for each dose level with the horizontal bar at the median. The limits of each box shows the inter-quartile range. The “notches” on each box indicates the 95% confidence interval on the median. The black dots represent outliers in the group and the vertical lines are valid limits of the data.

movements from series of flow run images, particularly with comparatively higher areal densities of interacting platelets. A recent and elegant paper by Chenouard and colleagues described an objective comparison of a panel of particle tracking methods and concluded that no single method was universally applicable due to inherent differences in the nature of the objects being tracked.⁴ In the case of tracking platelets in flow-based

assays, the nature of the objects being tracked does pose unique challenges: saltatory motion in a predominantly single direction along with complex merging/separation events. Prior methods have been prone to artifacts such as track fragmentation, and there has not been any comprehensive validation of the algorithms.^{6,7,21,24,26} We therefore set out in this study to determine systematic errors inherent in our

algorithms and metrics, and hence to find any limitations that will help to adapt future comparative platelet flow run comparisons that make use of our method. While we validated our algorithm using simulated data that represent platelet dynamics in a relatively simplistic manner, the approach provides a fundamental framework to model more complex platelet behavior in future development of the analysis software (available by request via the corresponding author).

Nevertheless, we have shown the utility of our current methodology and metrics in biological systems. The assay showed that the extent of platelet-vWF interaction is indeed correlated with platelet count, but other aspects of platelet behavior (e.g. translocating speed, relative level of stable adhesion) are largely similar among individuals with different platelet counts.

We then showed biologically-concordant changes in platelet properties by perturbation of platelet-vWF interactions. In the first instance we demonstrated treatment of donor blood with MRS2179, a P2Y₁ inhibitor, resulted in an increase in platelet translocation speed. While this increase was considerable, the other measured parameters did not change significantly after MRS2179 was administered. Furthermore this contrasts with previous results where P2Y₁ inhibition caused a near threefold increase in translocation speed,¹⁵ although that previous experiment used a shear rate twice that of our assay. A potential explanation for the apparent similarity between pre-treated and MRS2179-treated blood may be that inhibition of the P2Y₁ receptor has more notable downstream effects (i.e. reduction in platelet recruitment, aggregation) relative to what we currently measure (initial platelet-vWF interactions). Hence future versions of our algorithm should take into account downstream events such as platelet aggregation and thrombus formation.

Finally, the results from our *in vitro* studies involving AK2 and ReoPro, known inhibitors of the platelet GPIIb α and GPIIb/IIIa receptors, respectively, have shown detectable and expected changes across the seven metrics we derive to characterize platelet function and dynamics (see “Results” section). In some cases we showed that the metrics should not be examined in isolation. For example, while the reduction in the number of tracks induced by AK2 pointed to decreased levels of initial platelet-vWF interactions mediated by GPIIb α , the elevated number of tracks induced by ReoPro may be interpreted by itself as evidence of having the opposite effect, i.e. increased initial platelet-vWF interactions. Only when the adhesion rate is taken into account does the real picture emerge (Figs. 11 and 12). For AK2, the concomitant decrease in the adhesion rate does indeed point to reduced initial platelet-vWF interactions. But for ReoPro, the increased number of tracks along with

similar adhesion rates did not support the opposite effect but rather an observation of more platelet “traffic” owing to translocating platelets that were rolling faster and further compared to control. This is perhaps a powerful demonstration of how the assay, together with the metrics derived in this study, can be utilized to characterize platelet behavior. We have also elaborated on how the metrics relate to platelet function in a biological context (Table 2), in particular how they can reflect changes in the activities of key receptors (GPIIb and GPIIb/IIIa). In future studies, we anticipate that combinations of all or subsets of such metrics from our assay can be used to define profiles of pathological platelet behavior.

CONCLUSION

We have described the development and performance of novel tracking software that computes seven key metrics of platelet dynamics in flow-based assays. Extensive tests were carried out to validate this method and to reduce errors/artifacts. We have also demonstrated the utility of the software in detecting platelet property changes/differences in real biological systems, by administering known anti-platelet agents to whole human blood.

Using a large number of simulated datasets, we have shown that our tracking algorithm is effective in deriving seven key metrics that could be used to characterize platelet function. The major influence on the numbers of errors for each metric is the number of platelets being tracked. As the number of platelets increases, there are higher incidences of merging and separating platelets and, hence, mistracking events. Some metrics are affected more than others; weighted median speed is weakly influenced while determination of the number of stably-adhered platelets appears to be more heavily influenced.

Finally, our method was successfully used to analyze real flow run data from a series of experiments with confirmation of the expected biological outcomes. We demonstrated the ability of the assay to detect variation in platelet-vWF interactions as influenced by an individual’s platelet count.

By treating donor blood with a P2Y₁ antagonist (MRS2179) *in vitro* we showed an increase in platelet translocation speed, as expected. And while MRS2179 did not significantly affect many of the measured parameters. Our assay, currently focused on the early phase of platelet-vWF interactions, may not readily detect the more notable effects of P2Y₁ inhibition that happen in later phases, i.e. reduction in platelet recruitment and aggregation.

We then showed that *in vitro* introduction of a GPIIb inhibitor reduced the level of initial platelet-vWF

interactions and consequent signaling in a dosage dependent manner that are reflected by our measured parameters. Similarly we showed that *in vitro* administration of a GPIIb/IIIa inhibitor reduced stable platelet-vWF adhesion in a dosage dependent manner, as reflected across multiple parameters from the assay.

The results are encouraging for deployment of our validated flow-based system to characterize platelet functional differences between healthy and a range of disease cohorts, where our metrics will facilitate more powerful multi-parameter analysis.

ELECTRONIC SUPPLEMENTARY MATERIAL

The online version of this article (doi:[10.1007/s13239-016-0282-x](https://doi.org/10.1007/s13239-016-0282-x)) contains supplementary material, which is available to authorized users.

ACKNOWLEDGMENTS

This material is based upon work supported by Science Foundation Ireland under Grant No.10/CE/B1821.

CONFLICT OF INTEREST

A Ralph, M. Somers, J. Cowman, B. Voisin, E. Hogan, H. Dunne, E. Dunne, B. Byrne, N. Kent, A. Ricco, D. Kenny, and S. Wong declare that they have no conflict of interest.

STATEMENT OF HUMAN STUDIES

This study was approved by the Medical Research Ethics Committee of the Royal College of Surgeons in Ireland and complied with the Declaration of Helsinki.

STATEMENT OF ANIMAL STUDIES

No animal studies were carried out by the authors for this article.

REFERENCES

- ¹Andrews, R. K., J. López, and M. C. Berndt. Molecular mechanisms of platelet adhesion and activation. *Int. J. Biochem. Cell Biol.* 29:91–105, 1997.
- ²Andrews, R. K., Y. Shen, E. E. Gardiner, J. F. Dong, J. A. López, and M. C. Berndt. The glycoprotein Ib-IX-V complex in platelet adhesion and signaling. *Thromb. Haemost.* 82:357–364, 1999.
- ³Bryckaert, M., J.-P. Rosa, C. V. Denis, and P. J. Lenting. Of von Willebrand factor and platelets. *Cell. Mol. Life Sci.* 72:307–326, 2015.
- ⁴Chenouard, N., *et al.* Objective comparison of particle tracking methods. *Nat. Methods* 11:281–289, 2014.
- ⁵dos Meyer Santos, S., U. Klinkhardt, R. Schneppenheim, and S. Harder. Using ImageJ for the quantitative analysis of flow-based adhesion assays in real-time under physiologic flow conditions. *Platelets* 21:60–66, 2010.
- ⁶Gelles, J., B. J. Schnapp, and M. P. Sheetz. Tracking kinesin-driven movements with nanometre-scale precision. *Nature* 331:450–453, 1988.
- ⁷Ghosh, R. N., and W. W. Webb. Automated detection and tracking of individual and clustered cell surface low density lipoprotein receptor molecules. *Biophys. J.* 66:1301–1318, 1994.
- ⁸Ikeda, Y., M. Handa, K. Kawano, T. Kamata, M. Murata, Y. Araki, H. Anbo, Y. Kawai, K. Watanabe, and I. Itagaki. The role of von Willebrand factor and fibrinogen in platelet aggregation under varying shear stress. *J. Clin. Invest.* 87:1234–1240, 1991.
- ⁹Jackson, S. P. The growing complexity of platelet aggregation. *Blood* 109:5087–5095, 2007.
- ¹⁰Kent, N. J., L. Basabe-Desmots, G. Meade, B. D. MacCraith, B. G. Corcoran, D. Kenny, and A. J. Ricco. Microfluidic device to study arterial shear-mediated platelet-surface interactions in whole blood: reduced sample volumes and well-characterised protein surfaces. *Biomed. Microdevices* 12:987–1000, 2010.
- ¹¹Kroll, M. H., J. D. Hellums, L. V. McIntire, I. A. Schafer, and J. L. Moake. Platelets and shear stress. *Blood* 88:1525–1541, 1996.
- ¹²Kulkarni, S., S. M. Dopheide, C. L. Yap, C. Ravanat, M. Freund, P. Mangin, K. A. Heel, A. Street, I. S. Harper, F. Lanza, and S. P. Jackson. A revised model of platelet aggregation. *J. Clin. Invest.* 105:783–791, 2000.
- ¹³Lincoln, B., A. J. Ricco, N. J. Kent, L. Basabe-Desmots, L. P. Lee, B. D. MacCraith, D. Kenny, and G. Meade. Integrated system investigating shear-mediated platelet interactions with von Willebrand factor using microliters of whole blood. *Anal. Biochem.* 405:174–183, 2010.
- ¹⁴Lopez-Alonso, A., B. Jose, M. Somers, K. Egan, D. P. Foley, A. J. Ricco, S. Ramström, L. Basabe-Desmots, and D. Kenny. Individual platelet adhesion assay: measuring platelet function and antiplatelet therapies in whole blood via digital quantification of cell adhesion. *Anal. Chem.* 85:6497–6504, 2013.
- ¹⁵Mazzucato, M., M. R. Cozzi, P. Pradella, Z. M. Ruggeri, and L. De Marco. Distinct roles of ADP receptors in von Willebrand factor-mediated platelet signaling and activation under high flow. *Blood* 104:3221–3227, 2004.
- ¹⁶Otsu, N. A threshold selection method from gray-level histograms. *IEEE Trans. Syst. Man. Cybern.* 9:62–66, 1979.
- ¹⁷Perl, A., D. N. Reinhoudt, and J. Huskens. Microcontact printing: limitations and achievements. *Adv. Mater.* 21:2257–2268, 2009.
- ¹⁸R Development Core Team. R: A language and environment for statistical computing. R Foundation for Statistical Computing, Vienna, Austria. ISBN 3-900051-07-0, URL <http://www.R-project.org/>. *R Found. Stat. Comput. Vienna, Austria.*, 2012.
- ¹⁹Radmacher, M., M. Fritz, C. M. Kacher, J. P. Cleveland, and P. K. Hansma. Measuring the viscoelastic properties of human platelets with the atomic force microscope. *Biophys. J.* 70:556–567, 1996.
- ²⁰Ruggeri, Z. M. Platelets in atherothrombosis. *Nat. Med.* 8:1227–1234, 2002.

- ²¹Ruhnau, P., C. Guetter, T. Putze, and C. Schnörr. A variational approach for particle tracking velocimetry. *Meas. Sci. Technol.* 16:1449–1458, 2005.
- ²²Savage, B., F. Almus-Jacobs, and Z. M. Ruggeri. Specific synergy of multiple substrate-receptor interactions in platelet thrombus formation under flow. *Cell* 94:657–666, 1998.
- ²³Savage, B., E. Saldivar, and Z. M. Ruggeri. Initiation of platelet adhesion by arrest onto fibrinogen or translocation on von Willebrand factor. *Cell* 84:289–297, 1996.
- ²⁴Saxton, M. J., and K. Jacobson. Single-particle tracking: applications to membrane dynamics. *Annu. Rev. Biophys. Biomol. Struct.* 26:373–399, 1997.
- ²⁵Wickham, H. *ggplot2: Elegant Graphics for Data Analysis*. New York: Springer, 2009.
- ²⁶Work, S. S., and D. M. Warshaw. Computer-assisted tracking of actin filament motility. *Anal. Biochem.* 202:275–285, 1992.